Stochastic Thermodynamics in Mesoscopic Chemical Oscillation Systems

Tiejun Xiao,[‡] Zhonghuai Hou,*[,†,‡] and Houwen Xin[‡]

Hefei National Lab for Physical Science at Microscale, and Department of Chemical Physics, University of Science and Technology of China, Hefei, Anhui, 230026, People's Republic of China

Received: February 21, 2009; Revised Manuscript Received: April 3, 2009

Stochastic thermodynamics in mesoscopic chemical oscillation systems is discussed on the basis of chemical Langevin equation for the state variables with particular attention paid to a parameter region close to the deterministic Hopf bifurcation. The Langevin dynamics defines stochastic trajectories in the state space and therefore trajectory dependent entropy and entropy production according to the schemes proposed by Udo Seifert (*Phys. Rev. Lett.* **2005**, *95*, 040602). The total entropy change along a stochastic trajectory obeys the fluctuation theorems. By using the stochastic normal form theory, we derive explicit theoretical expressions for the mean entropy production in the stationary state. The resulting entropy production in the large system volume V limit can scale linearly or independent with V when the control parameter is above or below the Hopf bifurcation while it is of $V^{1/2}$ at the bifurcation. We verify the above relations by direct simulation with a stochastic circadian clock model.

1. Introduction

In recent years, nonequilibrium thermodynamics of small systems has gained extensive attention.[1,2] Of particular interest are the fluctuation theorems (FTs) for the general relations of the statistics of work, heat and, even far from equilibrium. The concept of FT was originally proposed by Evans et al. in multiparticle Hamiltonian systems.[3,4] Recently, it has been extended to more general stochastic dynamical systems described by Langevin or master equations.[5−18] In this context, an important progress known as stochastic thermodynamics (ST)[13,14] was made very recently by Udo Seifert, who defines entropy along a single stochastic trajectory. The total entropy change Δs_{tot} along a trajectory is found to be the logarithm of the probability ratio between the forward and backward paths. It also satisfies $\langle e^{-\Delta s_{tot}} \rangle = 1$ that can be related to the famous Jarzynski equality.[13] Generally, Δs_{tot} gives a trajectory-based measure of dynamic irreversibility.[19] It can also be related to thermodynamic heat and entropy production in stochastic systems, following an appropriate interpretation of the First Law.[14] ST has been successfully applied to a periodically modulated two-level system,[15] optically driven Brownian particles,[16] general chemical reaction networks,[17] and state transition process in biomolecules.[18]

We have recently applied the trajectory entropy approach to the study of the ST in a mesoscopic chemical oscillation system by the irreversible Brusselator model.[20] Here, the trajectory reversal can be realized in the discrete molecule−number state space that supports the master equation with the stochastic trajectories unraveled by the Gillespie algorithm.[21,22] We have calculated the entropy production P along a stochastic limit cycle in a parameter region close to the Hopf bifurcation (HB). The resulting P increases linearly with the system volume V in the deterministic oscillatory region, while it is independent with V in the steady state region. This study suggests a characteristic ST behavior in mesoscopic chemical bifurcation systems.

In this work, we exploit the similar approach to a mesoscopic reaction state space that supports chemical Langevin equation (CLE),[23] or equivalently, Fokker−Planck equation (FPE). The reversibility here requires only at a coarse grain level, much more relaxed than that in the molecule−number state space constructed in our previous work. The CLE defines stochastic trajectories in the concentration state space, sampled with a coarse-grained time scale. The mean entropy production P along a stochastic trajectory can be numerically calculated from the CLE by using path integral approach. Thanks to the stochastic normal form theory we developed recently,[24] explicit analytical expression for P is obtained when the system is close to the HB. The slow oscillatory motion on the two-dimensional center manifold dominates P, which is proportional to Vr_m^2 with r_m the most probable amplitude of the oscillation. The theory clearly shows that P in the large V limit can scale linearly or independent with V when the control parameter is above or below the HB and it is of $V^{1/2}$ at the bifurcation. Since the analysis is based on the normal form equations, the observed scaling relations are thus universal in mesoscopic oscillations systems, suggesting a much more solid physical background of the present study than that of our previous work. In addition, the same observations in our previous work and this study, though at different levels, shed some lights on the robustness of ST in characterization of bifurcation in mesoscopic systems. We have also verified above scaling relations by numerical simulation with a circadian clock model.

The paper is organized as follows. We present the CLE of mesoscopic reaction networks in Section 2. Stochastic thermodynamics associated with the CLE is discussed in section 3. By using normal form equations of the CLE, we derive theoretical expressions for the entropy production near the HB and discuss its scaling laws with the system size Vin section 4. Verification of the scaling laws in a circadian clock model is presented in section 5 followed by conclusion in the final section.

* To whom correspondence should be addressed. E-mail: hzhlj@ustc.edu.cn.

† Hefei National Lab for Physical Science at Microscale, University of Science and Technology of China.

‡ Department of Chemical Physics.

10.1021/jp901610x CCC: $40.75
Published on Web 06/11/2009

2. Model Description

We consider here a well-stirred mixture of N molecular species $\{S_1, ..., S_N\}$ that chemically interact inside some fixed volume V through M reaction channels ($R_1, ..., R_M$). We specify the dynamical state of this system by $\mathbf{X}(t) = (X_1(t), ..., X_N(t))^{\mathrm{T}}$ where $X_i(t)$ denotes the number of S_i molecules in the system at time t and the superscript "T" denotes transposition. We may write the reaction network in a compact form as

$$\{\mathbf{X} \rightarrow \mathbf{X} + \mathbf{v}_\rho\} \tag{1}$$

where $1 \leq \rho \leq M$ labels the single reaction channels, and $\mathbf{v}_\rho = (v_\rho^1, ..., v_\rho^N)^{\mathrm{T}}$ is the state change vector whose jth component v_ρ^j is defined as the change in the number of S_j molecules produced by one R_ρ reaction. Note that the forward and backward reactions of a reversible reaction are viewed as two separate channels in eq 1. In mesoscopic systems, the molecular populations $X_j(t)$ will be random variables. The transition probability $W_\rho(\mathbf{X})$ of R_ρ depends only on the current state and therefore defines a Markov process with a master equation

$$\partial_t P(\mathbf{X};t) = \sum_\rho [W_\rho(\mathbf{X} - \mathbf{v}_\rho)P(\mathbf{X} - \mathbf{v}_\rho;t) - W_\rho(\mathbf{X})P(\mathbf{X};t)] \tag{2}$$

governing the time evolution of the probability distribution $p(\mathbf{X};t)$ to have X_j molecules S_j at time t.

To account for the oscillation dynamics, we need to trace the dynamic evolution of $\mathbf{X}(t)$ in the state space with time. In practice, one can use Gillespie's algorithm to simulate the reaction processes by randomly determine what the next reaction is and when it will happen.[21,22] In addition, if a "macro-infinitesimal" time scale exists during which each reaction may take place many times and the transition rates do not change much, the dynamics can be well approximated by the following CLE

$$\frac{\mathrm{d}X_j}{\mathrm{d}t} = \sum_{\rho=1}^{M} v_\rho^j W_\rho(\mathbf{X}) + \sum_{\rho=1}^{M} v_\rho^j \sqrt{W_\rho(\mathbf{X})}\xi_\rho(t), \quad (j = 1, ..., N) \tag{3}$$

where $\xi_\rho = 1, ..., M(t)$ stand for independent Gaussian white noises associated with the reaction channels with $\langle \xi_\rho(t) \rangle = 0$ and $\langle \xi_\rho(t)\xi_{\rho'}(t') \rangle = \delta_{\rho\rho'}\delta(t - t')$. The validity of the CLE has been discussed in detail by Gillespie,[23] and generally speaking, it often applies to mesoscopic systems where the total populations of all species are very large compared to 1 or equivalently $V >> 1$. More commonly, eq 3 can be written in terms of the species concentrations $x_j(t) = X_j(t)/V$

$$\dot{x}_j = \sum_{\rho=1}^{M} v_\rho^j w_\rho(\mathbf{x}) + \frac{1}{\sqrt{V}} \sum_{\rho=1}^{M} v_\rho^j \sqrt{w_\rho(\mathbf{x})}\xi_\rho(t) \quad (j = 1, ..., N) \tag{4}$$

where $\mathbf{x} = (x_1, ..., x_N)^{\mathrm{T}}$ denotes the vector of concentrations and $w_\rho(\mathbf{x}) = W_\rho(\mathbf{x})/V$. In the thermodynamic limit $V \rightarrow \infty$, the CLE converges to a set of deterministic ordinary differential equations

$$\dot{x}_j = \sum_{\rho=1}^{M} v_\rho^j w_\rho(\mathbf{x}) \equiv f_j(\mathbf{x}) \quad (j = 1, ..., N) \tag{5}$$

which is essentially the macroscopic reaction rate equation of conventional chemical kinetics. The Fokker−Planck equation (FPE) corresponding to eq 4 reads

$$\frac{\partial p(\mathbf{x};t)}{\partial t} = -\sum_i \frac{\partial}{\partial x_i}[f_i(\mathbf{x})p(\mathbf{x};t)] + \frac{1}{2V}\sum_{i,j} \frac{\partial^2}{\partial x_i \partial x_j}[G_{ij}(\mathbf{x})p(\mathbf{x};t)] \tag{6}$$

where $p(\mathbf{x};t)$ is the probability distribution in the concentration space, $f_j(\mathbf{x})$ is the deterministic term defined in eq 5, and $G_{ij}(\mathbf{x}) = \sum_{\rho=1}^{M} v_\rho^i v_\rho^j w_\rho(\mathbf{x})$. By introducing probability current density

$$J_i(\mathbf{x}) = \frac{1}{2}\sum_j G_{ij}\left(H_j - \frac{1}{V}\frac{\partial}{\partial x_j}\right)p(\mathbf{x};t) \tag{7a}$$

where $H_j = 2\sum_k \Gamma_{jk}\tilde{f}_k$ with $\sum_j G_{ij}\Gamma_{jk} = \delta_{ik}$ and $\tilde{f}_k = f_k - 1/(2V)\sum_j(\partial G_{kj})/(\partial x_j)$, we can write the FPE in a compact form $\partial_t p(\mathbf{x};t) = -\sum_i(\partial J_i/\partial x_i)$. Note that eq 6 is consistent with the second-order Kramer-Moyal expansion of the master eq 2. We assume that the system (eq 6) admits a unique stationary distribution $p_s(\mathbf{x})$ with $\partial p_s(\mathbf{x};t)/\partial t = 0$. Throughout the present work, we will consider mesoscopic systems with $V >> 1$where the CLE and FPE are valid.

3. Stochastic Thermodynamics

We now consider a path $\chi(t) = \{\mathbf{x}(\tau)|_0^t\}$ generated by eq 4 starting from $\mathbf{x}_0(\tau = 0)$ selected from some normalized distribution $p_0(x_0)$ and ending at $\mathbf{x}_t(\tau = t)$ with normalized distribution $p_1(x_t)$. Correspondingly, the time-reversed path $\tilde{\chi}(t) = \{\tilde{\mathbf{x}}(\tau)|_0^t\}$, where $\tilde{\mathbf{x}}(\tau) = \mathbf{x}(t - \tau)$, starts from $\tilde{\mathbf{x}}_0 = \mathbf{x}_t$ and ends at $\tilde{\mathbf{x}}_t = \mathbf{x}_0$. According to Seifert,[15] one may define the entropy along this single trajectory as

$$s(\tau) = -\ln p(\mathbf{x}(\tau), \tau) \tag{7b}$$

where$p(\mathbf{x}(\tau),\tau)$is the solution of the Fokker−Planck equation evaluated along the trajectory at time τ. The rate of change of $s(\tau)$ is given by

$$\begin{aligned} \dot{s}(\tau) &= -\frac{\partial_t p(\mathbf{x},\tau)}{p(\mathbf{x},\tau)} - \frac{1}{p(\mathbf{x},\tau)}\sum_i \frac{\partial p(\mathbf{x},\tau)}{\partial x_i}\dot{x}_i \\ &= \left[-\frac{\partial_t p(\mathbf{x},\tau)}{p(\mathbf{x},\tau)} + \frac{2V}{p(\mathbf{x},\tau)}\sum_{ij}\Gamma_{ij}J_j\dot{x}_i\right] - V\sum_i H_i\dot{x}_i \end{aligned} \tag{8}$$

As shown in ref 13, the term in the square bracket in eq 8 denotes the trajectory-dependent total entropy production $\dot{s}_{\mathrm{tot}}(\tau)$ with balance $\dot{s}_{\mathrm{tot}}(\tau) = \dot{s}(\tau) + \dot{s}_{\mathrm{m}}(\tau)$, where

$$\dot{s}_{\mathrm{m}}(\tau) = V\sum_i H_i\dot{x}_i \tag{9}$$

is the "medium" entropy production.

Note that for a one-dimensional Langevin equation to describe the overdamped motion of a Brownian particle, $\dot{s}_{\mathrm{m}}(\tau)$ defined in this way can be related to the rate of heat dissipation in the medium.[13] For the currently system, $\dot{s}_{\mathrm{tot}}(\tau)$ and $\dot{s}_{\mathrm{m}}(\tau)$ are abstract quantities, and interpretations of them as exchanged heats are not feasible because the CLE (4) lacks an energetic interpretation.[14] However, the total entropy change along the trajectory, $\Delta s_{\mathrm{tot}} = \int_0^t \dot{s}_{\mathrm{tot}}(\tau)\mathrm{d}\tau$, is related to the so-called "dynamical irreversibility" or time asymmetry of the system.[19] According to path integral interpretation of the FPE (eq 6), the ratio of probabilities of the forward path $p[\chi(t)|\mathbf{x}_0]$ and the backward path $\tilde{p}[\tilde{\chi}(t)|\mathbf{x}_t]$ for given $\mathbf{x}_0$ and $\mathbf{x}_t$ can be calculated as[6]

$$\ln\frac{p[\chi(t)|\mathbf{x}_0]}{\tilde{p}[\tilde{\chi}(t)|\mathbf{x}_t]} = V\int_0^t \mathrm{d}t\sum_i H^i\dot{\mathbf{x}}_i = \Delta s_{\mathrm{m}} \tag{10}$$

which is the medium entropy change along the trajectory. Combine this quantity with the normalized distributions $p_0(\mathbf{x}_0)$ and $p_1(\mathbf{x}_t)$, we have

$$\ln \frac{p[\chi(t)]}{\tilde{p}[\tilde{\chi}(t)]} = \ln \frac{p[\chi(t)|\mathbf{x}_0]p_0(\mathbf{x}_0)}{\tilde{p}[\tilde{\chi}(t)|\mathbf{x}_t]p_1(\mathbf{x}_t)} = \Delta s_{\mathrm{m}} + \ln \frac{p_0(\mathbf{x}_0)}{p_1(\mathbf{x}_t)} \tag{11}$$

If $p_1(\mathbf{x}_t)$ is the solution of the FPE (eq 8) for the given initial distribution $p_0(\mathbf{x}_0)$, then $\ln(p_0(\mathbf{x}_0))/(p_1(\mathbf{x}_t)) = s(t) - s(0) = \Delta s$ is the system entropy change along the path, and the right-hand side of eq 11 is exactly Δs_{tot}.

From eq 11, one can obtain the following integral FT for the total entropy change Δs_{tot}[13]

$$\begin{aligned} \langle e^{-\Delta s_{\mathrm{tot}}} \rangle &\equiv \sum_{\mathbf{x}(\tau),\mathbf{x}_0} p[\chi(t)|\mathbf{x}_0]p_0(\mathbf{x}_0)e^{-\Delta s_{\mathrm{tot}}} \\ &= \sum_{\tilde{\mathbf{x}}(\tau),\tilde{\mathbf{x}}_0} p[\tilde{\chi}(t)|\tilde{\mathbf{x}}_0]p_1(\tilde{\mathbf{x}}_0) = 1 \end{aligned} \tag{12}$$

where we have used the fact that the summation over all forward paths is the same as that over all the backward ones. Equation 12 indicates $\langle \Delta s_{\mathrm{tot}} \rangle \geq 0$ which is in accordance with the second law. If the system stays in the stationary state and both $\mathbf{x}_0$ and $\mathbf{x}_t$ are chosen from $p_{\mathrm{s}}(\mathbf{x})$, then a stronger detailed FT also holds for Δs_{tot}[6,13]

$$p(\Delta s_{\mathrm{tot}})/p(-\Delta s_{\mathrm{tot}}) = e^{\Delta s_{\mathrm{tot}}} \tag{13}$$

We note that eqs 7 to 13 are extensions of Seifert's work to mesoscopic reaction systems on the level of CLE. Equation 9 gives the expression of medium entropy change which can be calculated by direct simulations of the CLE. Note that Δs is a boundary term and Δs_{m} increases monotonically with time such that $\Delta s_{\mathrm{tot}} \simeq \Delta s_{\mathrm{m}}$ in the long time run, hence eqs 12 and 13 also hold approximately for Δs_{m}. In the stationary state, we can also use the time-averaged entropy production P to measure the dynamic dissipation rate

$$P \equiv \lim_{t\to\infty} \frac{\langle \Delta S_{\mathrm{m}} \rangle}{t} = V \sum_i \langle\langle H_i \dot{\mathbf{x}}_i \rangle\rangle_{\mathrm{s}} \tag{14}$$

where $\langle\langle \cdot \rangle\rangle_{\mathrm{s}}$ means averaging over both time and the stationary distribution.

4. Entropy Production near Hopf Bifurcation: Theoretical Study

In this section, we investigate the properties of P associated with the oscillation dynamics of the system. We assume that the deterministic system (eq 5) has a unique steady state $\mathbf{x}_{\mathrm{s}}$ satisfying $f_i(\mathbf{x}_{\mathrm{s}}) = 0\ \forall i$, which loses stability at a supercritical HB$\mu = \mu_c$, where μ denotes the control parameter. Without lose of generality, we assume that sustained oscillation is observed in the superthreshold region $\mu > \mu_{\mathrm{c}}$. Generally, one cannot obtain the analytical expressions of Pdefined in eq 14, and one needs to perform numerical simulations of eq 4 to calculate P. However, thanks to the stochastic normal form theory we developed recently,[24] we find that theoretical analysis of P is possible close to the HB.

According to the Hopf theorem,[25] the Jacobian matrix $\mathbf{J}$ with entries $J_{ij} = (\partial f_i/\partial x_j)_{\mathbf{x}=\mathbf{x}_{\mathrm{s}}}$ has a pair of conjugate eigenvalues $\lambda_{\pm} = \alpha(\mu) \pm i\omega$ with $\alpha(\mu_c) = 0$. The other N-2 eigenvalues of $\mathbf{J}$, denoted by $-\lambda_{j(\geq 3)}$, all have strictly negative real parts with absolute values considerably larger than 0. By suitable variable transformations $\mathbf{u} = \mathbf{T}^{-1}(\mathbf{x} - \mathbf{x}_{\mathrm{s}})$, where the matrix $\mathbf{T}$ is derived from the eigenvectors of $\lambda_{\pm}$ and $-\lambda_{j(>3)}$, the linear part of eq 4 can be transformed to Jordan form and the equations for $\mathbf{u}$ read

$$\dot{\mathbf{u}} = \Lambda\mathbf{u} + O(\mathbf{u}^2) + \frac{1}{\sqrt{V}}\eta(t) \tag{15}$$

where the matrix

$$\Lambda = \begin{pmatrix} \alpha & -\omega \\ \omega & \alpha \end{pmatrix} \oplus \mathrm{diag}(-\lambda_3, ..., -\lambda_N)$$

is constructed by the eigenvalues. $\boldsymbol{\eta}(t) = \mathbf{T}^{-1}\boldsymbol{\zeta}(\mathbf{x}_{\mathrm{s}},t)$ denotes the vector of noise after transformation, where $\boldsymbol{\zeta} = (\zeta_1, ..., \zeta_N)^{\mathrm{T}}$ is the original noise vector involved in eq 4 with $\zeta_j(t) = \sum_\rho v_\rho^j (w_\rho(\mathbf{x}))^{1/2}\xi_\rho(t)$. The variances of $\boldsymbol{\eta}(t)$ are

$$\langle \eta_i(t)\eta_j(t') \rangle = 2D_{ij}\delta(t - t') \quad (i,j = 1, ..., N) \tag{16}$$

where D_{ij} is the entry of matrix $\mathbf{D} = \mathbf{T}^{-1}\mathbf{G}(\mathbf{T}^{-1})^{\mathrm{T}}$ with matrix $\mathbf{G}$ constructed from $G_{ij}(\mathbf{x}_{\mathrm{s}})$.

When the system (eq 15) locates near the HB such that $|\alpha| \ll 1$, the motion of the oscillatory mode related to (u_1,u_2) is much slower than the other N-2 stable modes, hence the system's dynamics will be dominated by the slow motion on a two-dimensional center manifold spanned by the eigenvectors of $\lambda_{\pm}$. The oscillatory modes are ruled by a normal form equation involving the time evolution of a complex variable $Z = u_1 + iu_2$, or a pair of coupled equations for the oscillation amplitude $r$and phase θ defined via $Z = re^{i\theta}$. By using the "stochastic averaging" method[26,27] and following the procedures in ref 24 we can obtain solvable "stochastic averaged normal forms" of the oscillatory mode as

$$\dot{r} = \alpha r + C_{\mathrm{r}}r^3 + \frac{\varepsilon^2}{2Vr} + \frac{\varepsilon}{\sqrt{V}}\eta_{\mathrm{r}}(t) \tag{17a}$$

$$\dot{\theta} = \omega + C_i r^2 + \frac{\varepsilon}{r\sqrt{V}}\eta_\theta(t) \tag{17b}$$

with $\varepsilon^2 = D_{11} + D_{22}$. $\eta_r(t)$ and $\eta_\theta(t)$ are temporally uncorrelated, statistically independent Gaussian white noises with unit variances. C_{r} and C_i are constants decided by the nonlinear terms in eq 15 evaluated at $\mathbf{x}_{\mathrm{s}}$. We can also calculate the normal forms of the remaining N-2 stable modes, which read

$$\dot{u}_j \simeq -\lambda_j u_j + \beta_j r^2 + \frac{1}{\sqrt{V}}\eta_j(t) \quad (j \geq 3) \tag{18}$$

where β_js are also constants. From eqs 17 and 18, we can get the stationary distribution as

$$p_{\mathrm{s}}(r, u_{j>2}) = N_1 e^{-\Phi(r)} \cdot N_2 e^{-\Psi(\mathbf{u})} \equiv p_{\mathrm{s}}(r) \cdot p_{\mathrm{s}}(\mathbf{u}) \tag{19}$$

where N_1,N_2 are normalization constants and

$$\Phi(r) = V\left(\frac{\alpha}{2}r^2 + \frac{C_r}{4}r^4\right)/\varepsilon^2 - \ln r \tag{20a}$$

$$\Psi(\mathbf{u}) = -\frac{V}{2}\sum_{j,k>2} \frac{(\lambda_j + \lambda_k)}{2D_{jk}}\left(u_j - \frac{\beta_j}{\lambda_j}r^2\right)\left(u_k - \frac{\beta_k}{\lambda_k}r^2\right) \tag{20b}$$

Note that the distribution of θ (mod 2π) is uniform inside $(0,2\pi)$ and is not included in eq 19. The distribution related to the stable modes is simply Gaussian, while that for oscillation amplitude r is strongly not.

After the linear transformation $\mathbf{x} = \mathbf{x}_{\mathrm{s}} + \mathbf{T}\mathbf{u}$, we could write the entropy production rate in terms of $\mathbf{u}$. By introducing vector notations $\tilde{\mathbf{f}} = (\tilde{f}_1, ..., \tilde{f}_N)^{\mathrm{T}}$and $\mathbf{H} = 2\boldsymbol{\Gamma}\tilde{\mathbf{f}}$ with $\boldsymbol{\Gamma} = \mathbf{G}^{-1}$, we have

$$P = V\langle\langle \mathbf{H}^{\mathrm{T}}\dot{\mathbf{x}} \rangle\rangle_{\mathrm{s}} = 2V\langle\langle \tilde{\mathbf{f}}^{\mathrm{T}}\Gamma^{\mathrm{T}}\dot{\mathbf{x}} \rangle\rangle_{\mathrm{s}} \simeq 2V\langle\langle \mathbf{u}^{\mathrm{T}}\mathbf{L}\dot{\mathbf{u}} \rangle\rangle_s \equiv 2V\sum_{ij} L_{ij}\langle\langle u_i\dot{u}_j \rangle\rangle_{\mathrm{s}} \tag{21}$$

where $\mathbf{L} \equiv \mathbf{T}^{\mathrm{T}}\mathbf{J}^{\mathrm{T}}\boldsymbol{\Gamma}^{\mathrm{T}}\mathbf{T}$. In the third equality, we have used

$$\tilde{\mathbf{f}}(\mathbf{x}) \simeq \mathbf{f}(\mathbf{x}) = \mathbf{f}(\mathbf{x}_s) + \mathbf{J}(\mathbf{x} - \mathbf{x}_s) + o(\left\|\left\|\mathbf{u}\right\|\right\|^2) \simeq \mathbf{JTu} \tag{22}$$

because $V \gg 1$, $\mathbf{f}(\mathbf{x}_s) = 0$, and $||\mathbf{u}|| \ll 1$. In the final equality of eq 21, the matrix elements L_{ij} are calculated at the fixed point $\mathbf{x}_s$ and thus can be taken out of the averaging brackets. Therefore, what we need to calculate are $h_{ij} \equiv \langle\langle u_i \dot{u}_j \rangle\rangle_s$. Note that in the stationary state, $(d/dt)\langle\langle u_i u_j \rangle\rangle_s = 0$, thus $h_{ij} \equiv \langle\langle u_i \dot{u}_j \rangle\rangle_s = -\langle\langle u_j \dot{u}_i \rangle\rangle_s \equiv -h_{ji}$ and $h_{ii} = 0$. From eqs 17 to 19, we have

$$\begin{aligned} h_{12} &\equiv \langle\langle u_1 \dot{u}_2 \rangle\rangle_s = -h_{21} = \left\langle\left\langle r\cos\theta \frac{d}{dt}(r\sin\theta)\right\rangle\right\rangle_s \\ &= \frac{1}{2\pi}\int_0^{2\pi} \cos^2\theta \, d\theta \cdot \int_0^{\infty} \dot{\theta} r^2 p_s(r) dr \simeq \frac{1}{2}\omega\langle r^2\rangle_s \end{aligned} \tag{23}$$

where we have substituted the time averaging by averaging over θ due to the oscillatory dynamics, and $\langle r^2\rangle_s \equiv \int_0^{\infty} r^2 p_s(r) dr$. Similarly, for $j > 2$

$$h_{1j} \equiv \langle\langle u_1 \dot{u}_j \rangle\rangle = \langle\langle r\cos\theta \dot{u}_j \rangle\rangle_s \simeq 0, \quad h_{2j} = \langle\langle r\sin\theta \dot{u}_j \rangle\rangle_s \simeq 0 \tag{24}$$

And for $j, k > 2$, after some manipulations, one can obtain

$$\begin{aligned} h_{kj} &\equiv \langle\langle u_k \dot{u}_j \rangle\rangle_s \simeq \langle\langle u_k[(-\lambda_j u_j + \beta_j r^2)]\rangle\rangle + \frac{1}{\sqrt{V}}\langle\langle u_k \eta_j(t)\rangle\rangle \\ &= \frac{-2\lambda_j}{\lambda_k + \lambda_j}\frac{D_{ij}}{V} + \frac{D_{ij}}{V} = \frac{\lambda_k - \lambda_j}{\lambda_k + \lambda_j}\frac{D_{kj}}{V} \end{aligned} \tag{25}$$

Combining eqs 21 and 23 to 25, we have

$$P = V(L_{12} - L_{21})\omega\langle r^2\rangle_s + 2\sum_{j,k>2} L_{kj} D_{kj} \frac{\lambda_k - \lambda_j}{\lambda_k + \lambda_j} \tag{26}$$

Equation 26 relates the average entropy production to the dynamic properties. To get more insight, we can approximate $\langle r^2\rangle_s$ by r_m^2, where r_m is the most probable value of r in the stationary state. By solving $\partial p_s(r)/\partial r|_{r_m} = 0$, one gets[24]

$$r_m^2 = (\sqrt{\alpha^2 - 2C_r\varepsilon^2/V} + \alpha)/(-2C_r) \tag{27}$$

An important result of eqs 26 and 27 is that the entropy production P shows different scaling with the system size V when the control parameter bypasses the HB. In the subthreshold region where $\alpha < 0$, $\lim_{V\to\infty} Vr_m^2 = \varepsilon^2/2|\alpha|$ and thus P is independent of V. At exactly the HB where $\alpha = 0$, $\lim_{V\to\infty} Vr_m^2 = [V\varepsilon^2/(-2C_r)]^{1/2} \propto V^{1/2}$, the term associated with the oscillatory mode dominates in eq 26, thus P scales as $V^{1/2}$. In the superthreshold region where $\alpha > 0$ and deterministic oscillation exists, $\lim_{V\to\infty} Vr_s^2 = V|\alpha|/(-C_r) \propto V$ and P scales as V^1. Therefore

$$\beta \equiv \lim_{V\to\infty} \frac{\ln P}{\ln V} = \begin{cases} 0 & \alpha < 0 \\ 1/2 & \alpha = 0 \\ 1 & \alpha > 0 \end{cases} \tag{28}$$

We note here that eq 28 establishes a relationship between the properties of stochastic entropy production and dynamic bifurcations in mesoscopic reaction systems. In the macroscopic limit, Hopf bifurcation can be clearly identified because the system's dynamics changes significantly when the control parameter passes through it. But in a mesoscopic system, molecular fluctuations smear the bifurcation and a clear identification of the HB is questionable. For instance, it was shown that the probability distributions in the phase space are qualitatively the same in both sides of the deterministic HB,[28] and dynamic behaviors are also nearly the same due to noise induced oscillations.[29,30] According to eq 28, the abrupt change in the scaling exponents in the large size limit clearly identifies the HB. It is also worthy to note here that only above the HB there is entropy production per volume associated with the limit cycle, that is, $P/V > 0$ for $V\to\infty$, while below the threshold, the system seems to be similar to a system in thermal equilibrium with no permanent current in the state space and hence no entropy production per volume, that is, $P/V = 0$ for $V\to\infty$.

TABLE 1: Reaction Channels Involved in the Circadian Clock Model

	reaction step	transition rate	description
1	$G \to R + G$	$w_1 = \upsilon_s k_I^n (k_I^n + x_3^n)^{-1}$	transcription
2	$R \to$	$w_2 = \upsilon_m x_1 (k_m + x_1)^{-1}$	R degradation
3	$R \to P_C + R$	$w_3 = k_s x_1$	translation
4	$P_C \to$	$w_4 = \upsilon_d x_2 (k_d + x_2)^{-1}$	degradation of P_C
5	$P_C \to P_N$	$w_5 = k_1 x_2$	transport of P_C into the nucleus
6	$P_N \to P_C$	$w_6 = k_2 x_3$	transport of P_N out of the nucleus

5. An Example: Circadian Clock Model

In this section, we will verify the main result derived above, eq 28, in a minimum circadian clock model. It is known that the molecular basis of the circadian clock involves genetic regulatory networks and internal noises often play important roles.[31,32] The model considered here incorporates the transcription of the gene (G) involved in the biochemical clock and transport of the mRNA (R) into the cytosol where it is translated into clock proteins (P_C) and degraded. The protein can be degraded or transported into the nucleus (P_N) where it exerts a negative regulation on the expression of its gene. According to these mechanisms, there are six reaction channels as listed in Table 1, where we have used $\mathbf{x} = (x_1, x_2, x_3)$ to stand for the concentrations of (R, P_C, P_N). υ_s denotes the transcription rate of mRNA, and we choose it as the control parameter. The other parameter values are $k_I = 2.0$ nM, Hill coefficient $n = 4$, maximum rate of mRNA degradation $\upsilon_m = 0.3$ nM h^{-1}, Michaelis constant related to mRNA degradation $k_m = 0.2$ nM, translation rate $k_s = 2.0$ h^{-1}, maximum rate of protein degradation $\upsilon_d = 1.5$ nM h^{-1}, Michaelis constant related to protein degradation $k_d = 0.1$ nM, transport rate $k_1 = k_2 = 0.2$ h^{-1}. According to these reaction steps, the stoichiometric matrix reads $\boldsymbol{\nu}_1 = (1\ -1\ 1\ 0\ 0\ 0)^T$, $\boldsymbol{\nu}_2 = (0\ 0\ -1\ -1\ -1\ 1)^T$, and $\boldsymbol{\nu}_3 = (0\ 0\ 0\ 0\ 1\ -1)^T$. The Langevin eq 4 can then be readily written down, where V can be interpreted as the effective cell volume. For these parameters, the HB locates at $\upsilon_s^{HB} \simeq 0.25725$, and other system dependent parameters calculated at the HB are $C_r \simeq -0.3474$, $C_i \simeq 0.5772$ and $\varepsilon^2 \simeq 0.3556$.

We numerically simulate the CLE by Euler methods with a time step 0.002. After long enough transition time, 10^5 trajectories with length $t = 1$ are used to calculate the medium entropy change Δs_m via eq 9. We choose three control parameter values $\upsilon_s = 0.25, 0.25725, 0.26$, which are below, at, and above the HB, respectively. The distributions of Δs_m for $V = 500$ are plotted in Figure 1, where strong non-Gaussian shapes are observed. It is obvious that $\langle \Delta s_m \rangle > 0$ and the probability of observing trajectories with negative Δs_m is fairly small. The dependence of $\ln[p(\Delta s_m)/p(-\Delta s_m)]$ drawn as a function of Δs_m is a straight line with slope 1 (not shown) as expected from the detailed FT (eq 13). We note here that the distribution of Δs_m

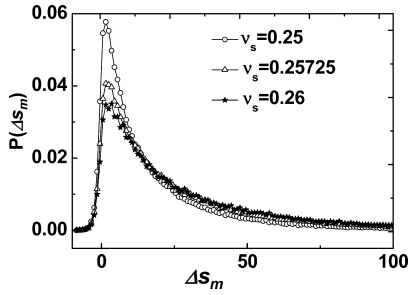

Figure 1. Distribution of the medium entropy change Δs_m. The shape does not change much when the bifurcation occurs.

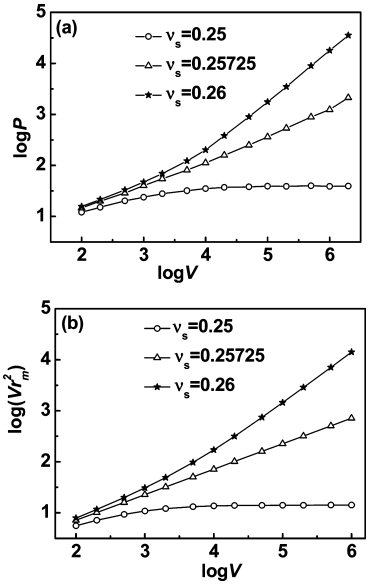

Figure 2. (a) Average entropy production $P \equiv \lim_{t\to\infty} \langle \Delta S_m \rangle / t$ for different system size V. The sampling time is $t = 10^5$. (b) Vr_m^2calculated from eq 27 is presented as a function of V. The lines are drawn to guide the eyes.

shows no significant difference at either side of the HB, and FT holds no matter the bifurcation happens or not.

In Figure 2a, the dependence of P on V is depicted. Here P is obtained from numerical simulation of the CLE according to eqs 9 and 14. Power-law scaling is observed in the large size limit, and the scaling exponents evaluated in the range $V \in [10^4,10^6]$are approximately 0.02, 0.53, and 0.98 for $v_s = 0.25$, 0.25725, 0.26, respectively, which are consistent with the theoretical values 0, 0.5, and 1.0. According to eq 26, the quantity $V\langle r^2 \rangle_s \simeq Vr_m^2$ dominates P. We have also calculated the theoretical values of Vr_m^2 according to eq 27, and its dependences on V are shown in Figure 2b, where the same scaling as that of P is apparent.

6. Conclusions

In summary, we have studied stochastic thermodynamics in mesoscopic chemical oscillation systems on the basis of chemical Langevin equations. Particular attention is paid to the properties of trajectory dependent entropy production near the Hopf bifurcation. By using the stochastic normal form theory, we have obtained the theoretical expression for the entropy production, which is a function of the system size, the oscillation amplitude and frequency, as well as other dynamic properties. In addition, we find that the entropy production scales asV^β in the large V limit with β changing abruptly from 0 to 1 when the control parameter bypasses the Hopf bifurcation, suggesting a way to characterize nonequilibrium phase transition in mesoscopic systems with stochastic thermodynamics behaviors. We verify our theoretical analysis by direct simulations of the chemical Langevin equation with a stochastic circadian clock model. Since the analysis is on the Langevin level, the results of the present work could apply to general mesoscopic oscillation reactions whether they are reversible or not.

Acknowledgment. The work is supported by the National Science Foundation of China (Grants 20673106, 20873130). The authors gratefully acknowledge many enlightening discussions with Professor Y. J. Yan.

References and Notes

(1) Bustamante, C.; Liphardt, J.; Ritort, F. *Phys. Today* **2005**, *58* (7), 43.
(2) Ritort, F. *J. Phys.: Condens. Matter.* **2006**, *18*, R531.
(3) Evans, D. J.; Cohen, E. G. D.; Morriss, G. P. *Phys. Rev. Lett.* **1993**, *71*, 2401.
(4) Evans, D. J.; Searles, D. J. *Phys. Rev. E* **1994**, *50*, 1645.
(5) Lebowitz, J. L.; Spohn, H. *J. Stat. Phys.* **1999**, *95*, 333.
(6) Chernyak, V. Y.; Chertkov, M.; Jarzynski, C. *J. Stat. Mech.: Theory Exp.* **2006**, 08001.
(7) Seifert, U. *J. Phys. A: Math. Theor.* **2004**, *37*, L517.
(8) Gaspard, P. *J. Chem. Phys.* **2004**, *120*, 8898.
(9) Andrieux, D.; Gaspard, P. *J. Chem. Phys.* **2004**, *121*, 6167.
(10) Andrieux, D.; Gaspard, P. *J. Stat. Mech: Theory Exp.* **2006**, 01011.
(11) Andrieux, D.; Gaspard, P. *J. Chem. Phys.* **2008**, *128*, 154506.
(12) Andrieux, D.; Gaspard, P. *Phys. Rev. E* **2008**, *77*, 031137.
(13) Seifert, U. *Phys. Rev. Lett.* **2005**, *95*, 040602.
(14) Seifert, U. *Eur. Phys. J. B* **2008**, *64*, 423.
(15) Tietz, C.; Schuler, S.; Speck, T.; Seifert, U.; Wrachtrup, J. *Phys. Rev. Lett.* **2006**, *97*, 050602.
(16) Blickle, V.; Speck, T.; Helden, L.; Seifert, U.; Bechinger, C. *Phys. Rev. Lett.* **2006**, *96*, 070603.
(17) Schmiedl, T.; Seifert, U. *J. Chem. Phys.* **2007**, *126*, 044101.
(18) Schmiedl, T.; Speck, T.; Seifert, U. *J. Stat. Phys.* **2007**, *128*, 77.
(19) Andrieux, D.; Ciliberto, S.; Garnier, N.; Joubaud, S.; Petrosyan, A. *Phys. Rev. Lett.* **2007**, *98*, 150601.
(20) Xiao, T. J.; Hou, Z.; Xin, H. *J. Chem. Phys.* **2008**, *129*, 114506.
(21) Gillespie, D. T. *J. Comput. Phys.* **1976**, *22*, 403.
(22) Gillespie, D. T. *J. Phys. Chem.* **1977**, *81*, 2340.
(23) Gillespie, D. T. *J. Chem. Phys.* **2000**, *113*, 297.
(24) Xiao, T.; Ma, J.; Hou, Z.; Xin, H. *New J. Phys.* **2007**, *9*, 403.
(25) Hassard, B. D.; Wan, Y. H. *Theory and Applications of Hopf bifurcation*, London Mathematical Society Lecture Note Series; Cambridge: Cambridge University Press, 1981; Vol. 4.
(26) Arnold, L.; Namachchivaya, N. S.; Schenk-Hoppé, K. R. *Int. J. Bifurcat. Chaos* **1996**, (6), 1947.
(27) Roberts, J. B.; Spanos, P. D. *J. Nonlinear Mech.* **1986**, *21*, 111.
(28) Qian, H.; Saffarian, S.; Elson, E. L. *Proc. Natl. Acad. Sci. U.S.A.* **2002**, *99*, 10376.
(29) Hou, Z.; Xin, H. *J. Chem. Phys.* **2003**, *119*, 11508.
(30) Hou, Z.; Xin, H. *ChemPhysChem.* **2004**, *5*, 407.
(31) Gonze, D.; Halloy, J.; Goldbeter, A. *Proc. Natl Acad. Sci. USA.* **2002**, *99*, 673.
(32) Gonze, D.; Hallory, J.; Gaspard, P. *J. Chem. Phys.* **2002**, *116*, 10997.

JP901610X